Planar and three-dimensional retrograde periodic orbits of asteroids

THOMAS A. KOTOULAS
and
GEORGE VOYATZIS

Aristotle University of Thessaloniki, Greece
Department of Physics,
Section of Astrophysics, Astronomy and Mechanics
Post Code:54124, P.O Box:102
E-mail address: tkoto@physics.auth.gr

30^{Ο} ΘΕΡΙΝΟ ΣΧΟΛΕΙΟ—ΣΥΝΕΔΡΟ: ΔΥΝΑΜΙΚΑ ΣΥΣΤΗΜΑΤΑ ΚΑΙ ΠΟΛΥΠΛΟΚΟΤΗΤΑ (28/8-6/9/2024)

ΛΙΣΤΑ ΑΣΤΕΡΟΕΙΔΩΝ

Appendix A: Additional table

Table A.1. Asteroids in RMMRs with planets.

Designation	a (au)	e	i	U	RMMR	n (f)	S	Resonant angle	k	Configurations
2015 BZ509	5.137	0.391	163.0	2	1/−1J	10 (100%)	10.00	Lib.at 180	1	Currently in RMMR
2000 DG8	10.76	0.794	129.3	4	1/−3J*	10 (100%)	10.00	Lib.at 0	0	Currently in RMMR
2011 KT19	35.58	0.331	110.1	2	7/−9N	10 (100%)	10.00	Lib.at 180	6	Currently in polar RMMR
2006 RJ2	9.675	0.762	164.6	7	2/−5J 1/−1S	7 (38.9%) 10 (90.9%)	2.723 9.090	Lib.at 180 Lib.at 0	2 0	Capture in RMMR Currently in RMMR
2018 DO4	25.75	0.907	160.5	4	1/−11J*	10 (90.9%)	9.090	Lib.at 0	0	Capture in RMMR
2012 YO6	6.317	0.478	106.9	4	3/−4J*	10 (88.2%)	8.820	Lib.at 180	3	Capture in polar RMMR
2005 NP82	5.870	0.478	130.5	1	5/−6J*	10 (87.3%)	8.730	Lib.at 180	4	Currently in RMMR
2011 MM4	21.13	0.473	100.5	4	3/−10S 5/−3N	10 (83.6%) 3 (36.3%)	8.360 1.089	Lib.at 180 Lib.at 180	3 4	Currently in polar RMMR Capture in polar RMMR
2008 KV42	41.50	0.491	103.4	3	8/−13N	10 (83.6%)	8.360	Lib.at 180	6	Capture in polar RMMR
2013 NS11	12.65	0.787	130.3	2	2/−3S*	10 (78.2%)	7.820	Lib.at 180	0	Capture in RMMR
2009 QY6	12.47	0.835	137.6	4	2/−3S	10 (77.3%)	7.730	Lib.at 180	0	Currently in RMMR
2016 LS	13.34	0.608	114.3	4	1/−4J* 3/−5S*	9 (81.8%) 5 (13.6%)	7.362 0.680	Lib.at 180 Lib.at 180	1 2	Currently in RMMR Capture in RMMR
2016 JK24	13.05	0.660	152.3	3	1/−4J*	8 (81.8%)	6.544	Lib.at 180	2	Capture in RMMR
2016 PN66	31.46	0.908	105.1	3	1/−15J*	8 (81.8%)	6.544	Lib.at 0	0	Capture in polar RMMR
2017 SV13	9.682	0.793	113.2	6	2/−5J 1/−1S	4 (19.1%) 9 (68.2%)	0.764 6.138	Lib.at 180 Lib.at 0	3 0	Capture in RMMR Currently in RMMR
2009 HC82	2.527	0.807	154.4	0	3/−1J*	7 (83.3%)	5.831	Lib.at 180	1	Capture in RMMR
1999 LE31	8.135	0.466	151.8	3	1/−2J* 7/−1N*	8 (68.2%) 8 (68.2%)	5.456 5.456	Lib.at 0 Lib.at 0	0 0	Capture in RMMR Capture in RMMR
2008 YB3	11.63	0.440	105.1	1	3/−10J	10 (54.5%)	5.450	Lib.at 180	3	Currently in polar RMMR
2016 NM56	73.50	0.794	161.7	2	3/−11N*	10 (45.5%)	4.550	Lib.at 180	4	Capture in RMMR
2012 YF8	9.380	0.592	136.1	7	2/−5J 3/−7J* 1/−1S	6 (23.9%) 4 (22.3%) 6 (68.2%)	1.434 0.892 4.092	Lib.at 180 Lib.at 180 Lib.at 0	0 2 0	Capture in RMMR Capture in RMMR Capture in RMMR
2015 AO44	22.15	0.836	140.0	2	5/−6U*	4 (83.6%)	3.344	Lib.at 180	5	Capture in RMMR
2008 SO218	8.112	0.565	170.3	2	1/−2J 7/−1N*	6 (47.3%) 8 (36.4%)	2.838 2.912	Lib.at 180 Lib.at 180	1 4	Currently in RMMR Capture in RMMR
2006 BZ8	9.606	0.803	165.3	2	2/−5J 1/−1S	8 (33.7%) 3 (11.4%)	2.696 0.342	Lib.at 180 Lib.at 0	0 0	Currently in RMMR Capture in RMMR
2014 AT28	10.93	0.404	165.6	3	1/−3J*	4 (54.5%)	2.180	Lib.at 180	0	Capture in RMMR
2016 FH13	24.55	0.615	93.5	3	9/−13U*	4 (54.5%)	2.180	Lib.at 180	5	Capture in polar RMMR
2015 XX351	14.61	0.851	159.1	3	3/−14J*	3 (62.6%)	1.878	Lib.at 180	3	Capture in RMMR
2012 TL139	30.14	0.883	160.0	7	1/−14J*	8 (21.4%)	1.712	Lib.at 0	0	Currently in RMMR
2009 YS6	20.18	0.921	147.8	2	1/−3S*	3 (54.5%)	1.635	Lib.at 180	2	Capture in RMMR
2016 VY17	11.20	0.851	148.4	2	4/−13J*	9 (17.7%)	1.593	Lib.at 0	0	Capture in RMMR
2014 SQ339	28.66	0.903	128.5	7	1/−13J* 6/−11U*	8 (18.3%) 5 (13.9%)	1.464 0.695	Lib.at 180 Lib.at 180	2 1	Capture in RMMR Capture in RMMR
2016 TK2	9.180	0.552	92.3	4	3/−7J*	6 (21.4%)	1.284	Lib.at 180	2	Capture in polar RMMR
2011 SP25	19.58	0.884	109.0	6	1/−3S*	4 (32.1%)	1.284	Lib.at 0	0	Capture in polar RMMR
2005 TJ50	9.240	0.589	110.2	7	3/−7J* 1/−1S*	7 (18.2%) 1 (16.9%)	1.274 0.169	Lib.at 180 Lib.at 0	3 0	Capture in polar RMMR Currently in polar RMMR
2017 NM2	14.67	0.625	101.3	4	3/−14J*	3 (36.4%)	1.092	Lib.at 180	3	Capture in polar RMMR
2017 QO33	34.55	0.857	148.8	4	1/−7S* 4/−5N*	3 (27.3%) 2 (31.8%)	0.819 0.636	Lib.at 180 Lib.at 180	2 4	Capture in RMMR Capture in RMMR
2017 UX51	30.26	0.749	90.5	5	1/−14J*	3 (13.6%)	0.408	Lib.at 180	2	Currently in polar RMMR
2016 YB13	5.460	0.408	139.7	2	13/−5S*	2 (19.1%)	0.382	Lib.at 0	0	Capture in RMMR
2016 TP93	7.479	0.560	138.3	7	4/−1U*	1 (13.6%)	0.136	Lib.at 0	1	Capture in RMMR

Notes. The orbital elements and condition codes U are taken from the website of the JPL Small-Body Database Search Engine, retrieved on 10 April 2019. In the sixth column J, S, U, and N are acronyms of Jupiter, Saturn, Uranus, and Neptune, respectively. The asterisk indicates the original results. The value of the seventh column n presents the number of clones (including the nominal one) that are trapped in this RMMR. The data given in the parentheses f are longest times that the resonant clones remain trapped in corresponding RMMR relative to the whole integration time-span (−10 000 to 100 000 yr). Resonant status S and resonant angle ϕ are defined as in Eqs. (3) and (2), respectively. The parameter k of the resonant angle is also indicated. The last column shows whether an asteroid is currently in RMMR or will be captured in RMMR in our numerical calculation. Objects are ordered by their resonant status from high to low S. If an asteroid evolves in several RMMRs, we sort it according to the best resonant status.

Outline

- Framework : Restricted 3-body problem (RTBP)
- Study : 1st, 2nd and 3rd order MMRs with Jupiter
- Method: Computation of families of Periodic Orbits and Stability
- Other methods: Averaged Hamiltonian, Mapping models, Simulations
- Hierarchy of models: Planar Circular, Elliptic, 3D Circular or Elliptic RTBP

We study periodic orbits because:

-they critically determine the phase-space structure

-equilibrium points of averaged Hamiltonian

-KAM theory→stable POs are associated with invariant tori in phase space

-other applications to the extrasolar planetary systems (**Antoniadou and Voyatzis, 2013 & 2014**)

The Lagrangian of the system

$$\mathcal{L}_R = \frac{1}{2}(\dot{x}^2 + \dot{y}^2 + \dot{z}^2) + (x\dot{y} - y\dot{x})\dot{\upsilon} + \frac{1}{2}(x^2 + y^2)\dot{\upsilon}^2 + \frac{1-\mu}{r_0} + \frac{\mu}{r_1}$$

$$r_0 = \sqrt{(x + \mu r_{01})^2 + y^2 + z^2}, \quad r_1 = \sqrt{(x - (1-\mu)r_{01})^2 + y^2 + z^2}$$

$\upsilon = \upsilon(t)$: *true anomaly and* $r_{01} =$
$= r_{01}(t)$ *is the mutual distance of the primaries along their Keplerian orbit*

$z = \dot{z} = 0 \Rightarrow$ *planar elliptic problem,*
$\dot{\upsilon} = 1$ *and* $r_{01} = 1$
$\Rightarrow$ *Circular problem (Jacobi integral)*

Equations of motion

- $$\left\{\begin{array}{c} \ddot{x} - 2\dot{y}\dot{v} - y\ddot{v} - x\dot{v}^2 = -(1-\mu)\frac{x+\mu}{r_0^3} - \mu\frac{x-1+\mu}{r_1^3}, \\ \ddot{y} + 2\dot{x}\dot{v} + x\ddot{v} - y\dot{v}^2 = -(1-\mu)\frac{y}{r_0^3} - \mu\frac{y}{r_1^3}, \\ \ddot{z} = -(1-\mu)\frac{z}{r_0^3} - \mu\frac{z}{r_1^3}. \end{array}\right\}$$

Planar Circular RTBP

- **Classical Configuration**: Rotating Oxy orthogonal system
- Sun, Jupiter as primaries ($\mu = 0.001,\ T = 2\pi$)
- Symmetry: $\Sigma: (t, x, y) \rightarrow (-t, x, -y)$
- **Direct orbit**: the minor body revolves around the Sun in the same direction as that of the primary body, e.g. Jupiter (with respect to the inertial frame)
- **Retrograde orbit**: the minor body revolves around the Sun in the opposite direction as that of the primary body, e.g. Jupiter (with respect to the inertial frame)

Families of periodic orbits

- **First kind**: $e \approx 0$, $({}^{n}/_{n'})$ varies along the family (circular orbits)
- **Second kind**: $e \neq 0, ({}^{n}/_{n'}) \approx const.$ (elliptic orbits)
- General characteristics for retrograde orbits:
- First kind: The family R_C is continued for $\mu \neq 0$ in all cases of resonances.
- Second kind:
- Family $R_I \rightarrow$ ***stable***; except for a small area where a close encounter with Jupiter occurs in some cases.
- Family $R_{II} \rightarrow$ *unstable*; a perpendicular collision orbit with Jupiter occurs when $a(1 + e) = 1$; then becomes stable.

Initial conditions: $x(0) = x_0, y(0) = 0, \dot{x}(0) = 0, \dot{y}(0) = \dot{y}_0.$

$\phi = q\lambda - p\lambda' - (p+q)\omega, \lambda = \mathrm{M} + \omega, R_I\colon \phi = 0, R_{II}\colon \phi = \pi.$

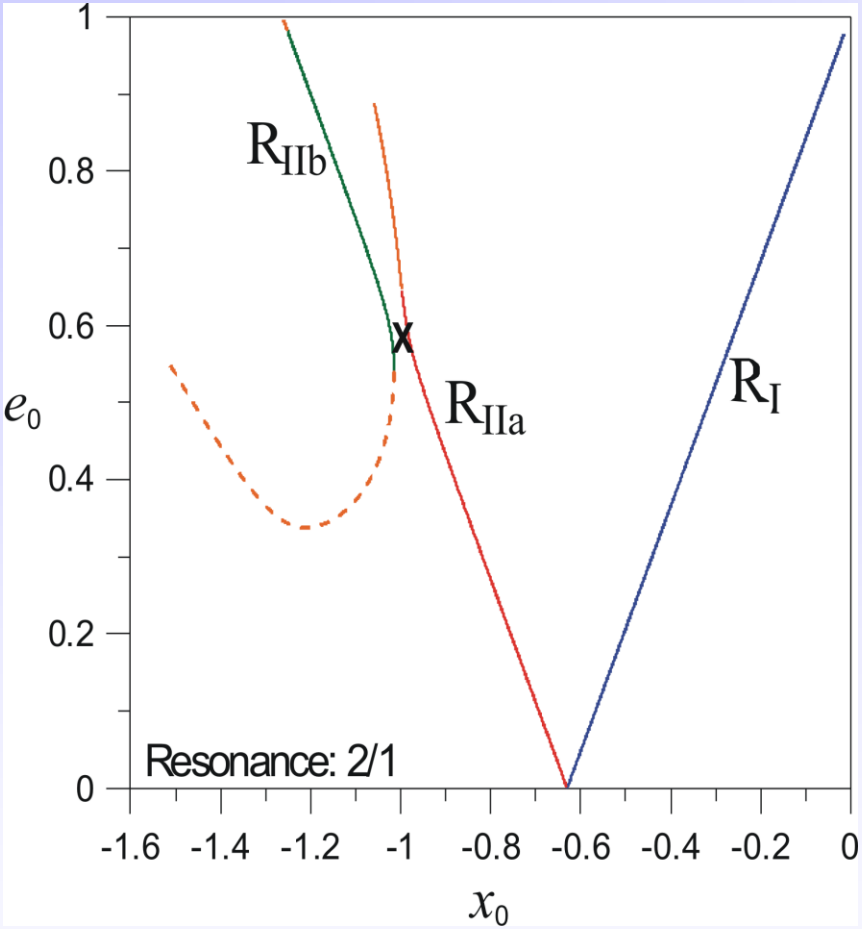

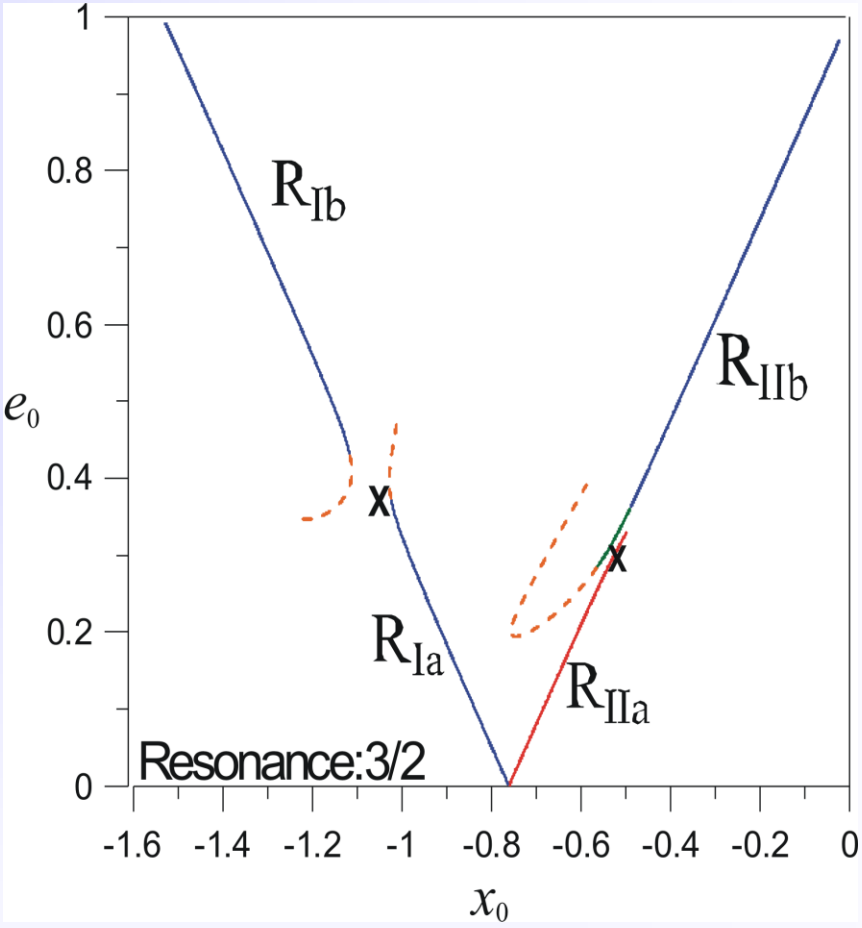

Comments : **blue** color→horizontal and vertical stability, **red**→horizontal instability but vertical stability, **green**→horizontal stability and vertical instability,
orange→horizontal and vertical instability // **x** →Collision orbit
(Kotoulas and Voyatzis, 2020a)

2nd order resonances: 3/1, 5/3, 7/5

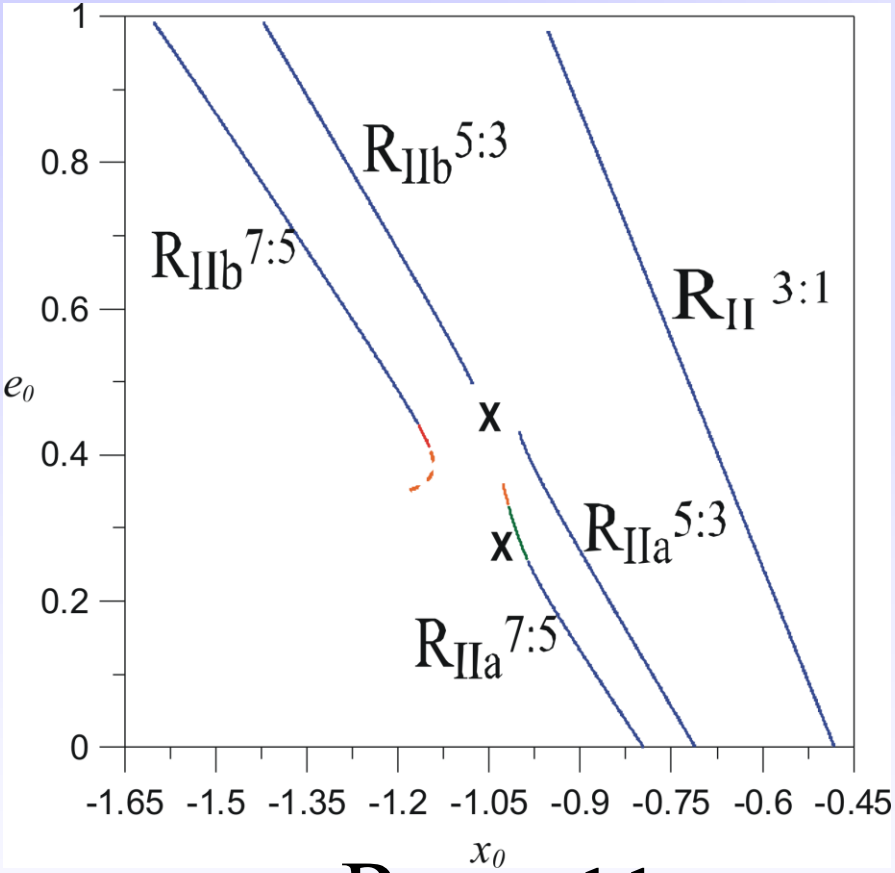

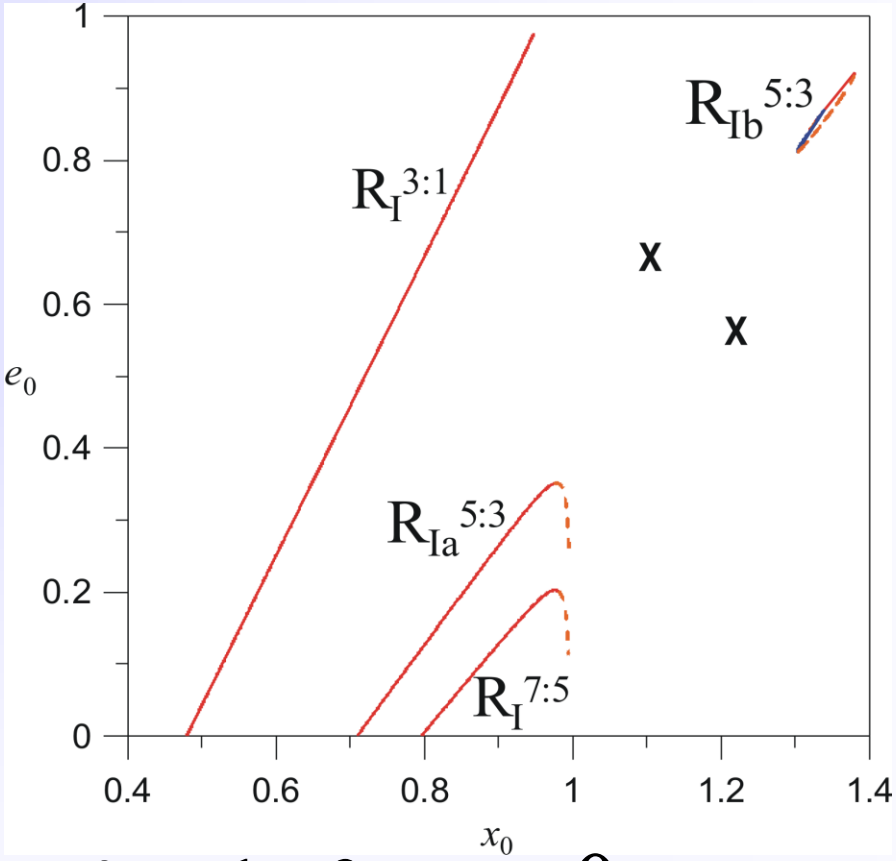

R_{II}: stable, $(dx/dt)_0=0$ only for $x_0<0$,

R_I: unstable, $(dx/dt)_0=0$ only for $x_0>0$.

3rd order resonances

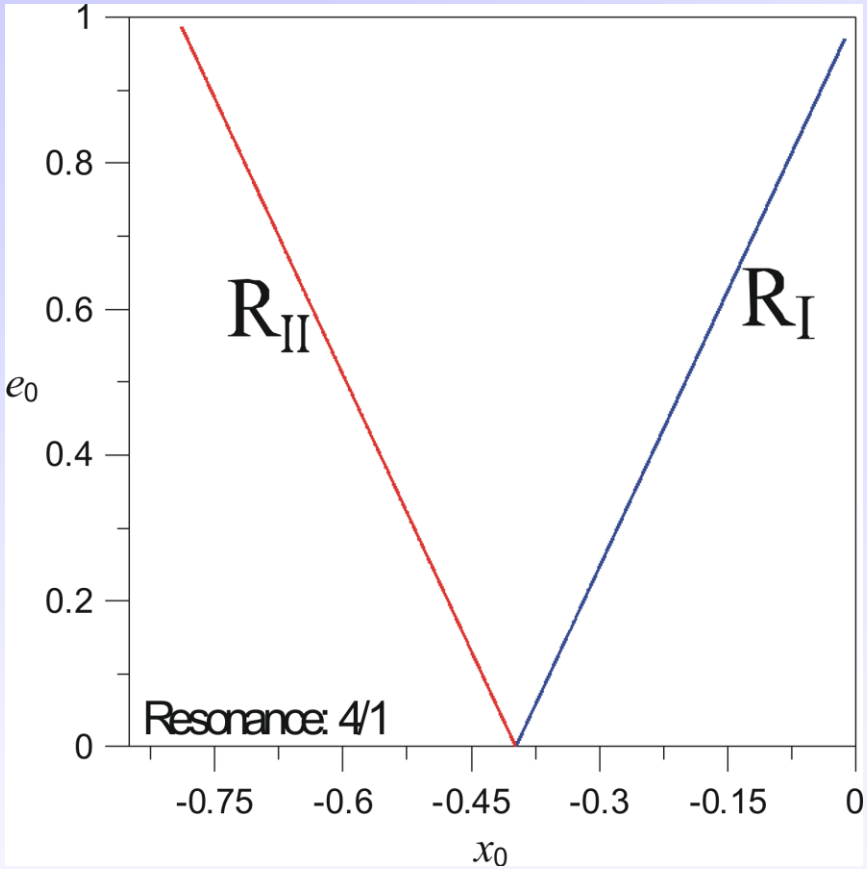

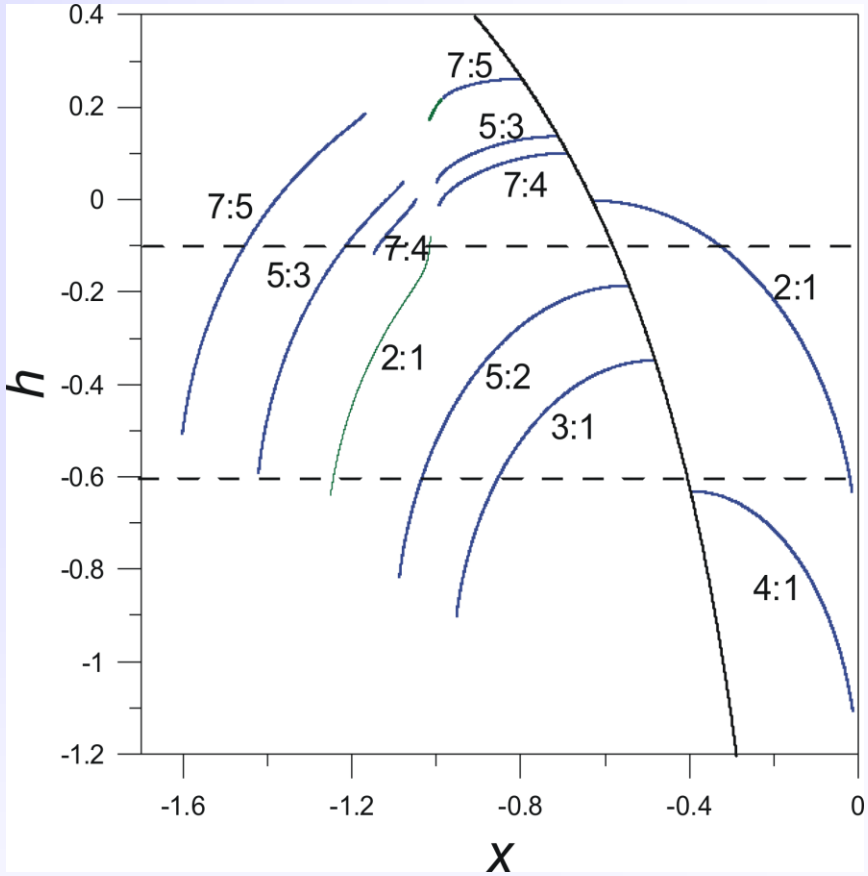

Comments : blue color→horizontal and vertical stability,
red→horizontal instability but vertical stability //

x →Collision orbit

Poincaré surface of section (y=0, dy/dt>0)
h=-0.6, h=-0.1

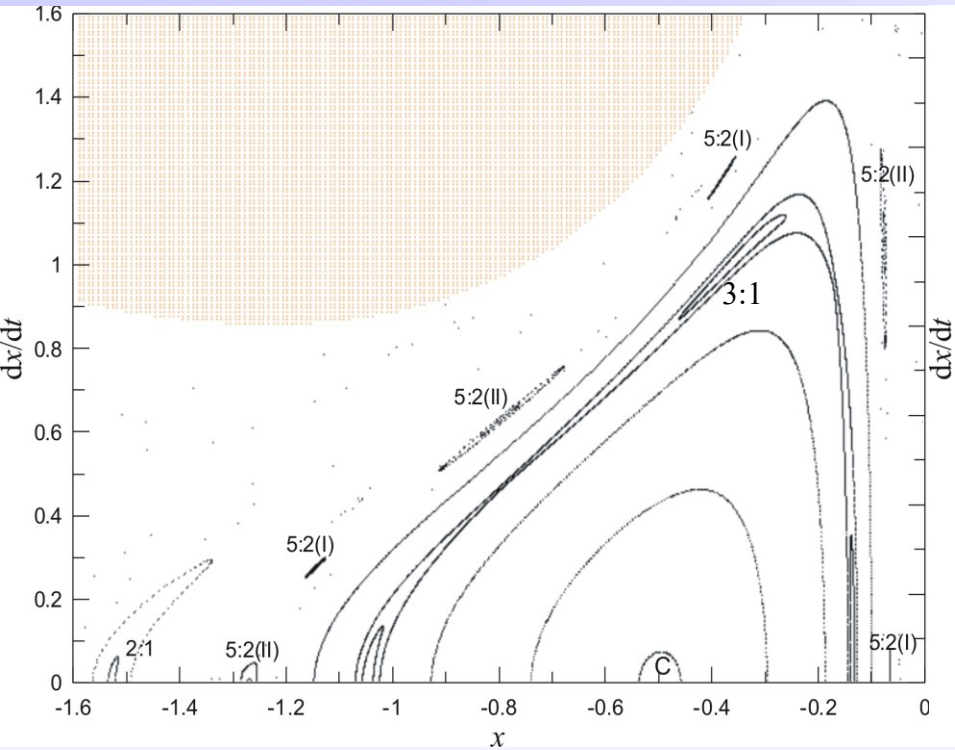

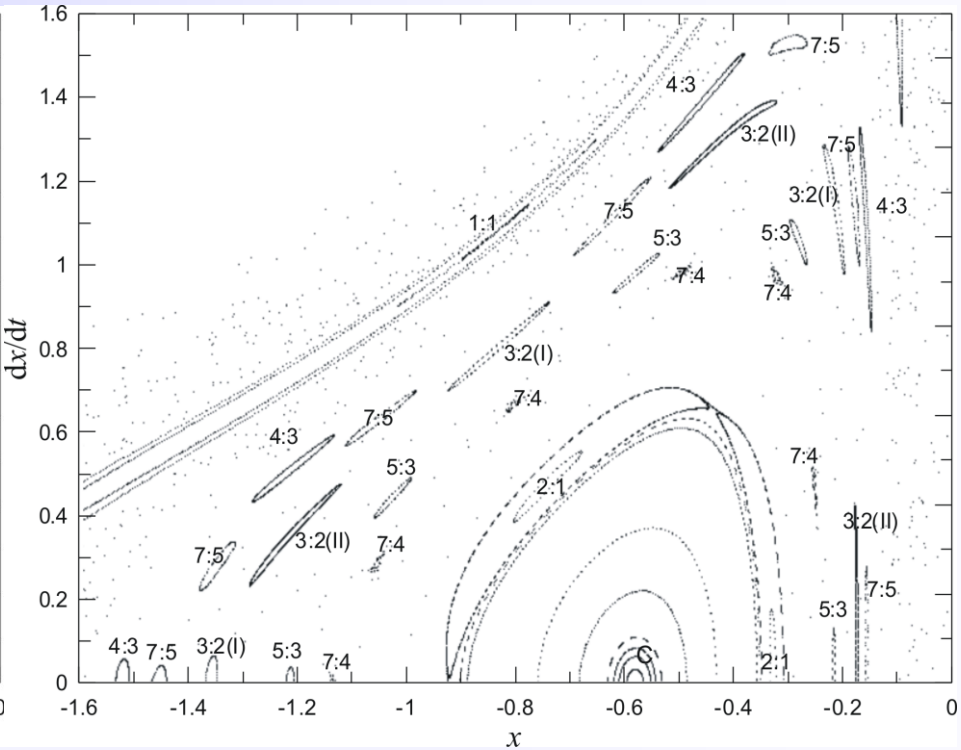

Number of islands=multiplicity of orbits=p+q, $\left({}^{n}/_{n'}\right) \cong \frac{p}{q}$.

(Kotoulas and Voyatzis: 2020a, PSS **182** (104846))

Elliptic RTBP: Families of symmetric POs

Bifurcation Points:Periodic Orbits of the 2-D Circular RTBP with T=2mπ, m ∈ ***Z***

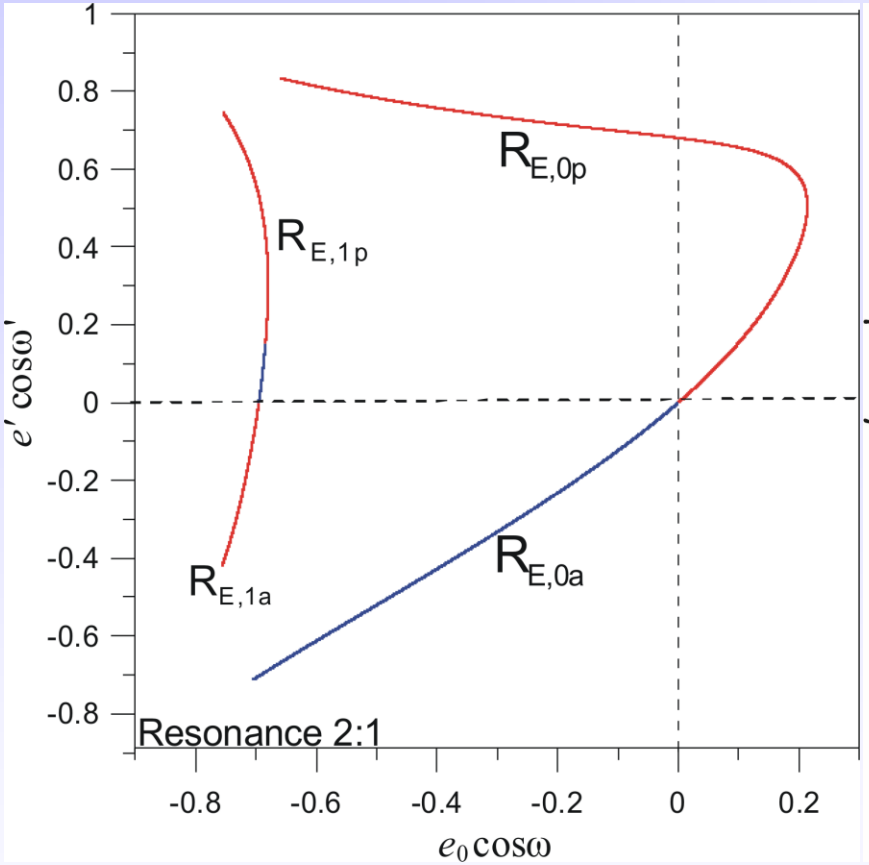

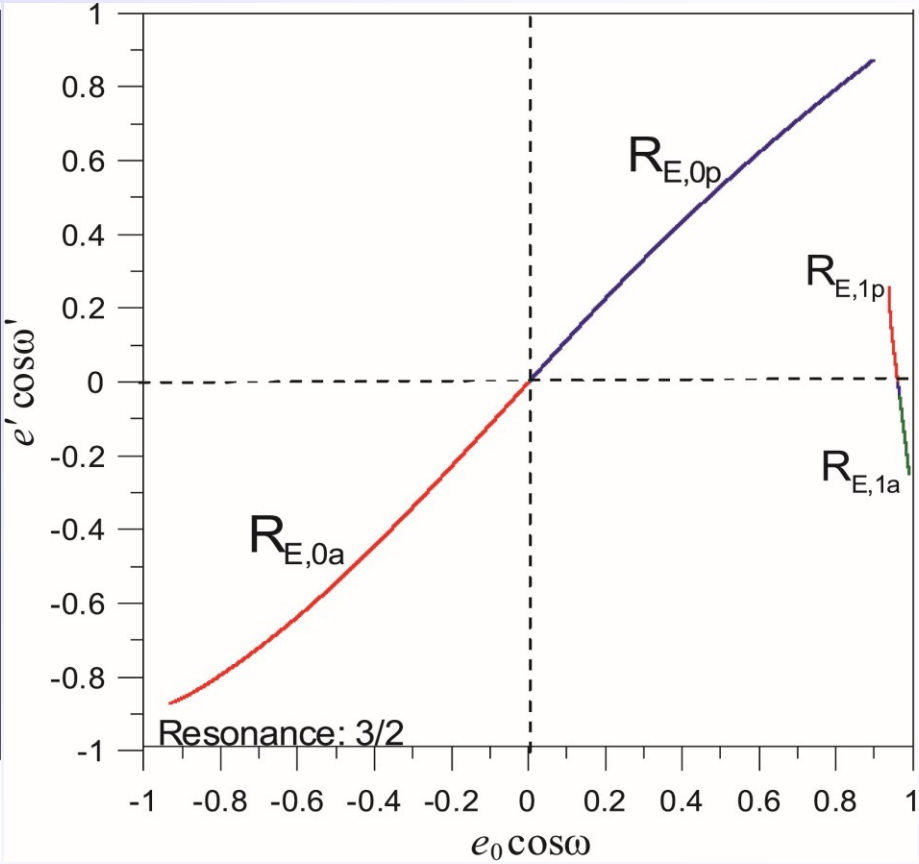

2 families form each point: Jupiter at perihelion (ω'=0) and Jupiter at aphelion (ω'=π).

p→ asteroid at perihelion, a→ asteroid at aphelion

Second order resonances

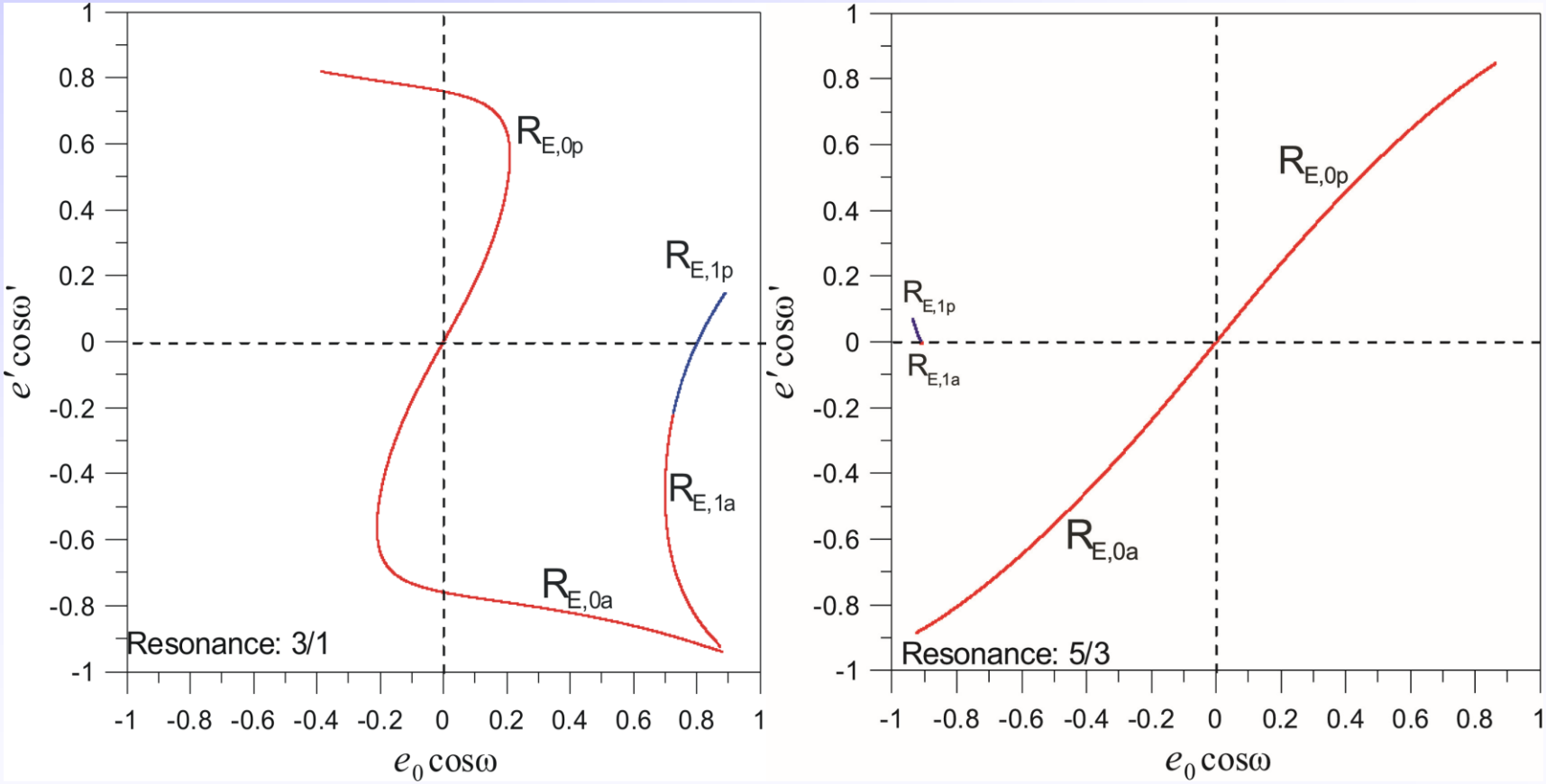

Third order resonances

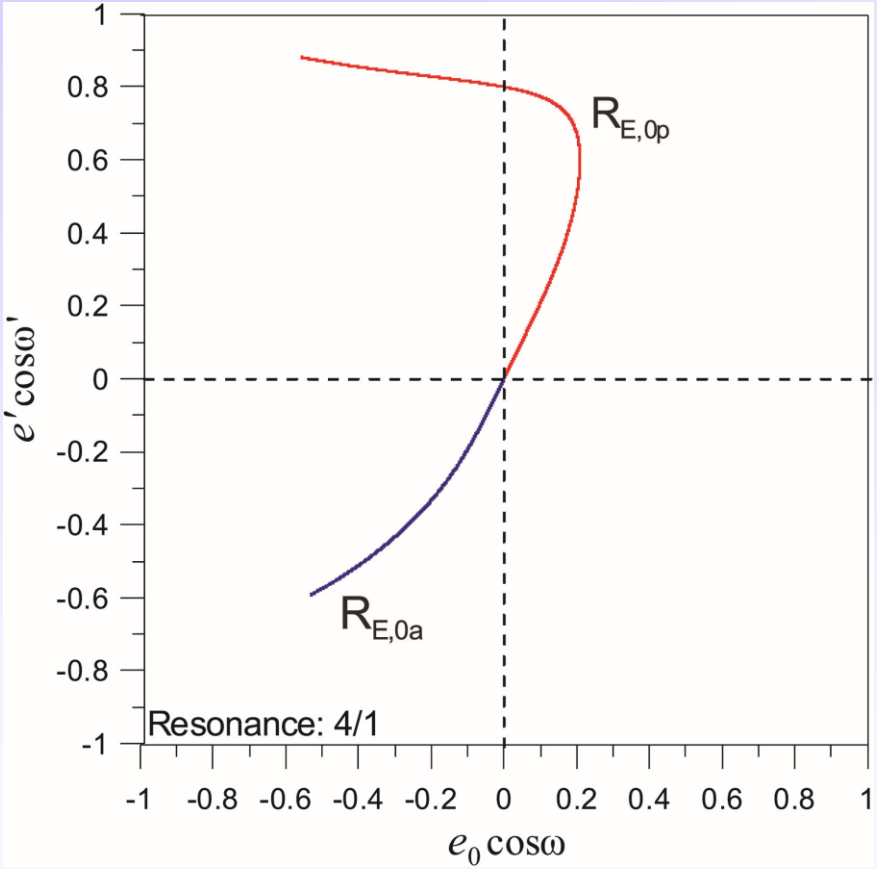

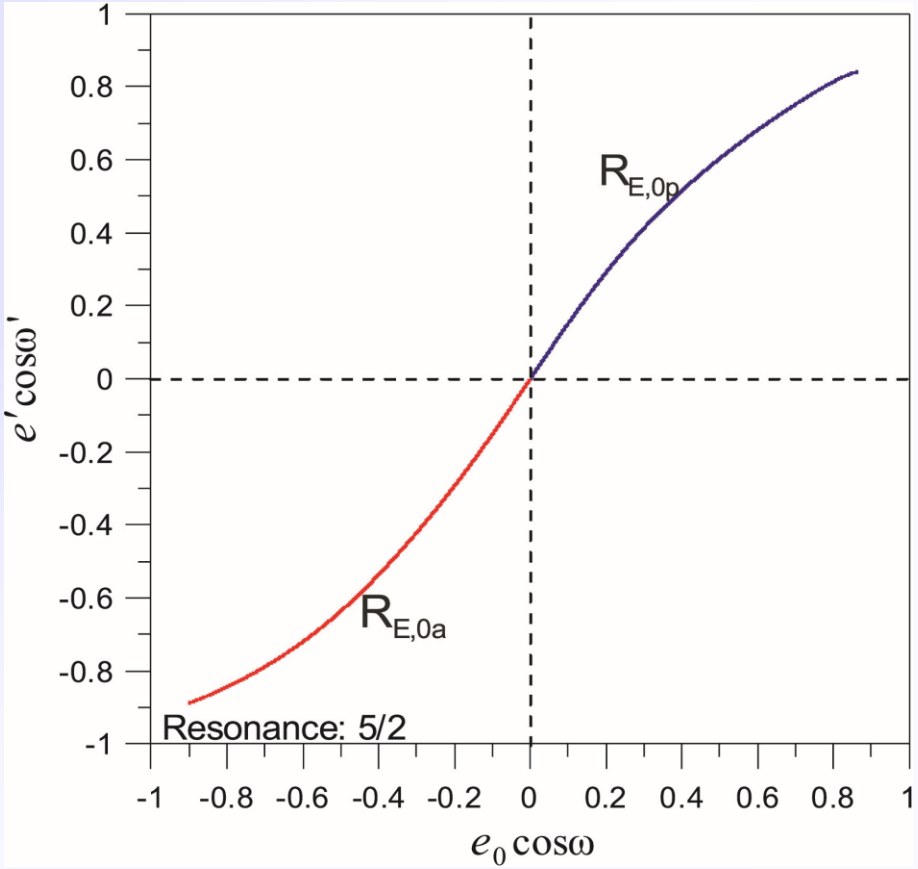

3-D Circular RTBP

Bifurcation Points: Periodic orbits of the planar circular problem with vertical critical stability **(Henon, 1973)**

- **Periodic orbits**: 1)F-symmetry with respect to *xz*—plane
  2)G-symmetry with respect to *x*-axis.
- Initial conditions:
- 1) $x(0) = x_0,\ y(0) = 0,\ z(0) = z_0,$
  $\dot{x}(0) = 0,\quad \dot{y}(0) = \dot{y}_0, \dot{z}(0) = 0.$
- 2) $x(0) = x_0,\ y(0) = 0,\ z(0) = 0,$
  $\dot{x}(0) = 0,\quad \dot{y}(0) = \dot{y}_0, \dot{z}(0) = \dot{z}_0.$

$(x_0, y_0, z_0, \dot{x}_0, \dot{y}_0, \dot{z}_0) \longrightarrow (\mathrm{a}, \mathrm{e}, i, \omega, M, \Omega)$

3-D Circular RTBP (a~const., e-i plane)

2/1 Resonance

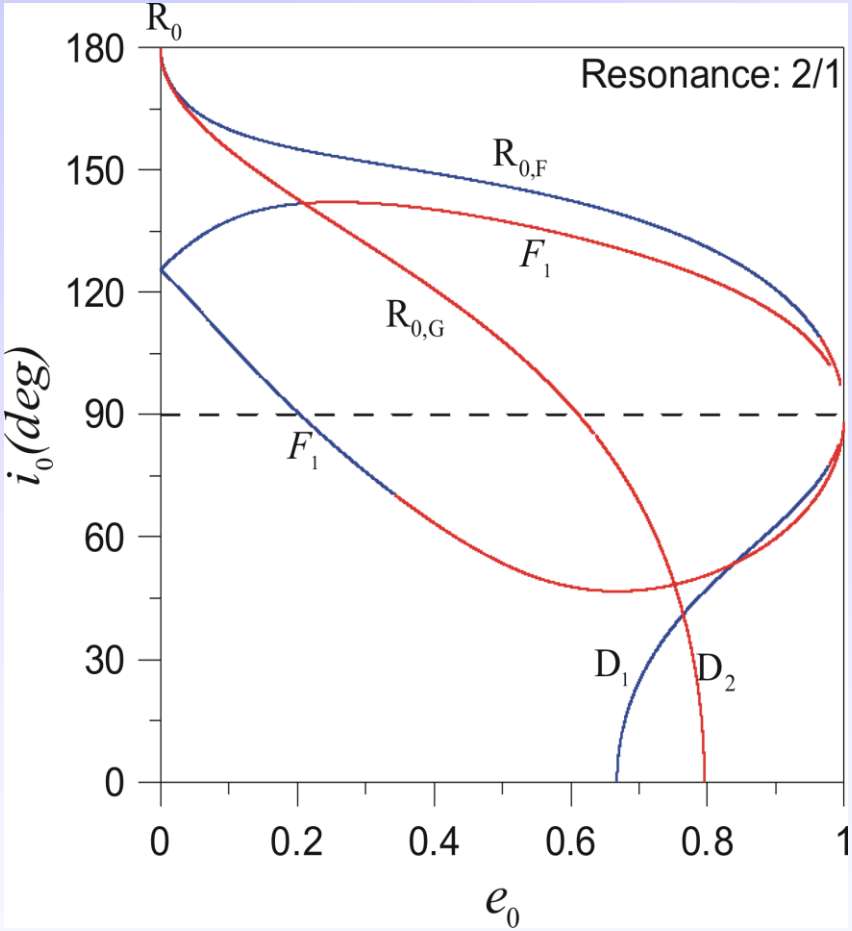

3/2 Resonance

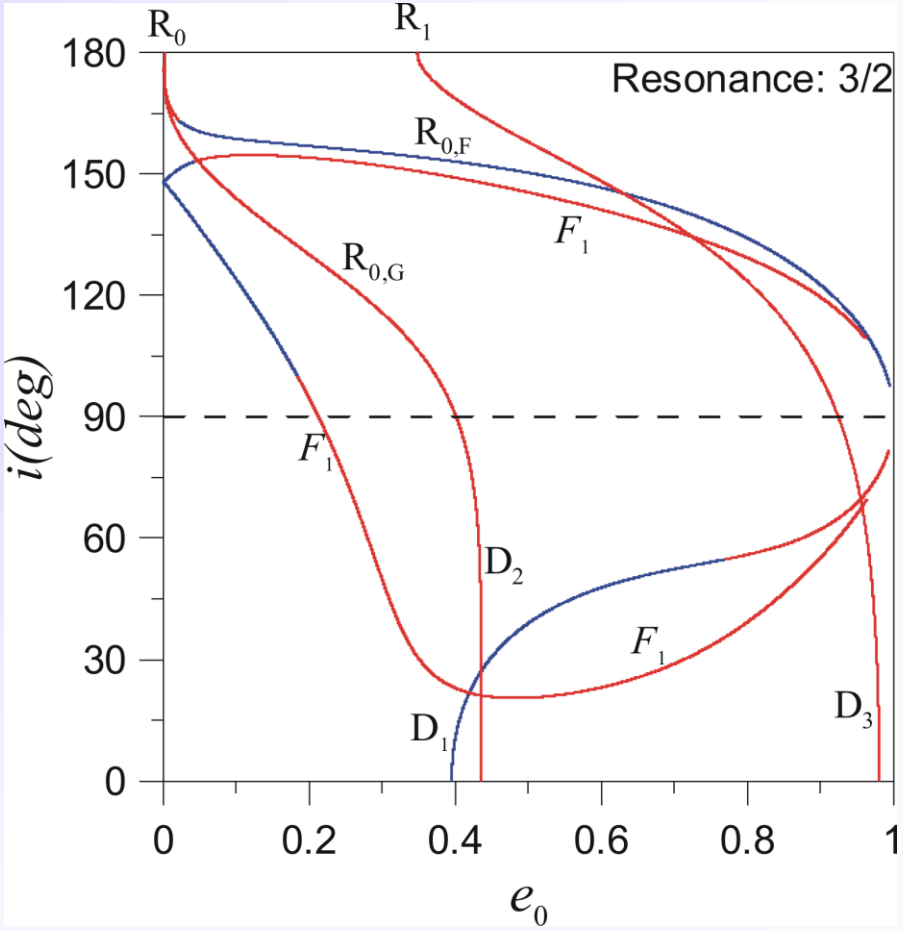

D: direct orbits $\{\varphi=q\lambda-p\lambda'+(p-q)\varpi, \varphi_z = q\lambda - p\lambda' + (p-q)\boldsymbol{\Omega}\}$,

R: retrograde orbits $\{\varphi=q\lambda-p\lambda'-(p+q)\varpi, \varphi_z = q\lambda - p\lambda' + (p+q)\boldsymbol{\Omega}\}$

blue colour→horizontal stability, red colour→horizontal instability

3/1 Resonance: Projection of these families of POs on *i*-*e* plane

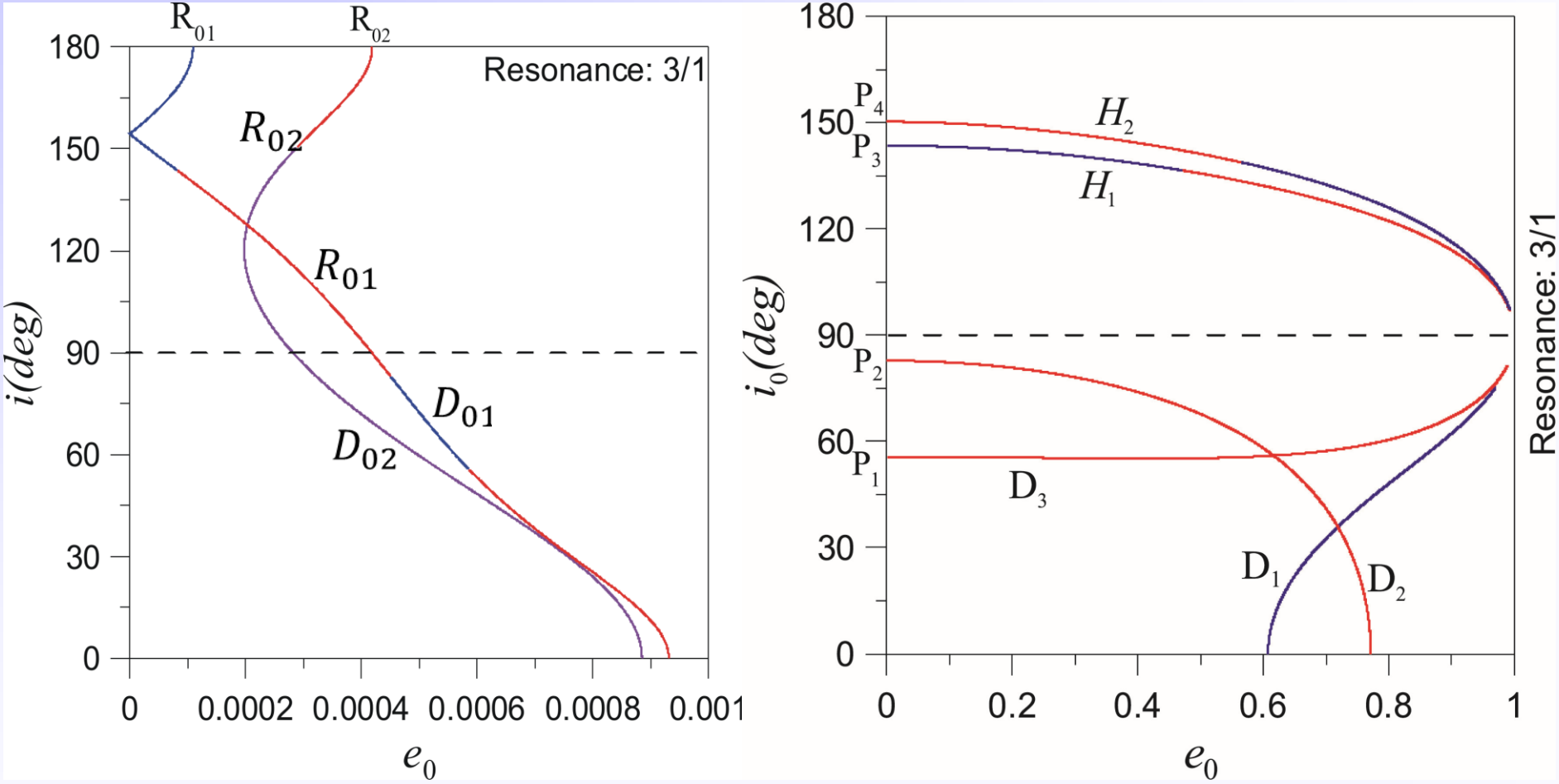

Blue colour→stability, red colour→instability, **magenta**→double instability
(Kotoulas, Voyatzis and M.H.M. Morais: 2022a, PSS **210** (105374))

2009 HC82

Element	Value	Uncertainty (1-sigma)	Units
e	0.8065122675266817	4.8522E-8	
a	2.527415739646448	4.3193E-8	**au**
q	0.4890239404815657	1.2228E-7	**au**
i	154.3609837251317	7.9081E-6	**deg**
node	295.4620693521495	2.0789E-5	**deg**
peri	298.9593485523253	1.8877E-5	**deg**
M	202.0579669165575	1.6062E-5	**deg**
tp	2460644.385550035899 2024-Nov-29.88555004	7.5316E-5	**TDB**
period	1467.619439155009 4.018123036700914	3.7622E-5 1.0300e-7	**d** **y**
n	0.2452951973757395	6.2881E-9	**deg/d**
Q	4.56580753881133	7.8029E-8	**au**

Dynamical stability maps (for 3/1 resonance)
(a) ω=Ω=270, M=180 deg, (b) ω=270, Ω=90, M=180 deg

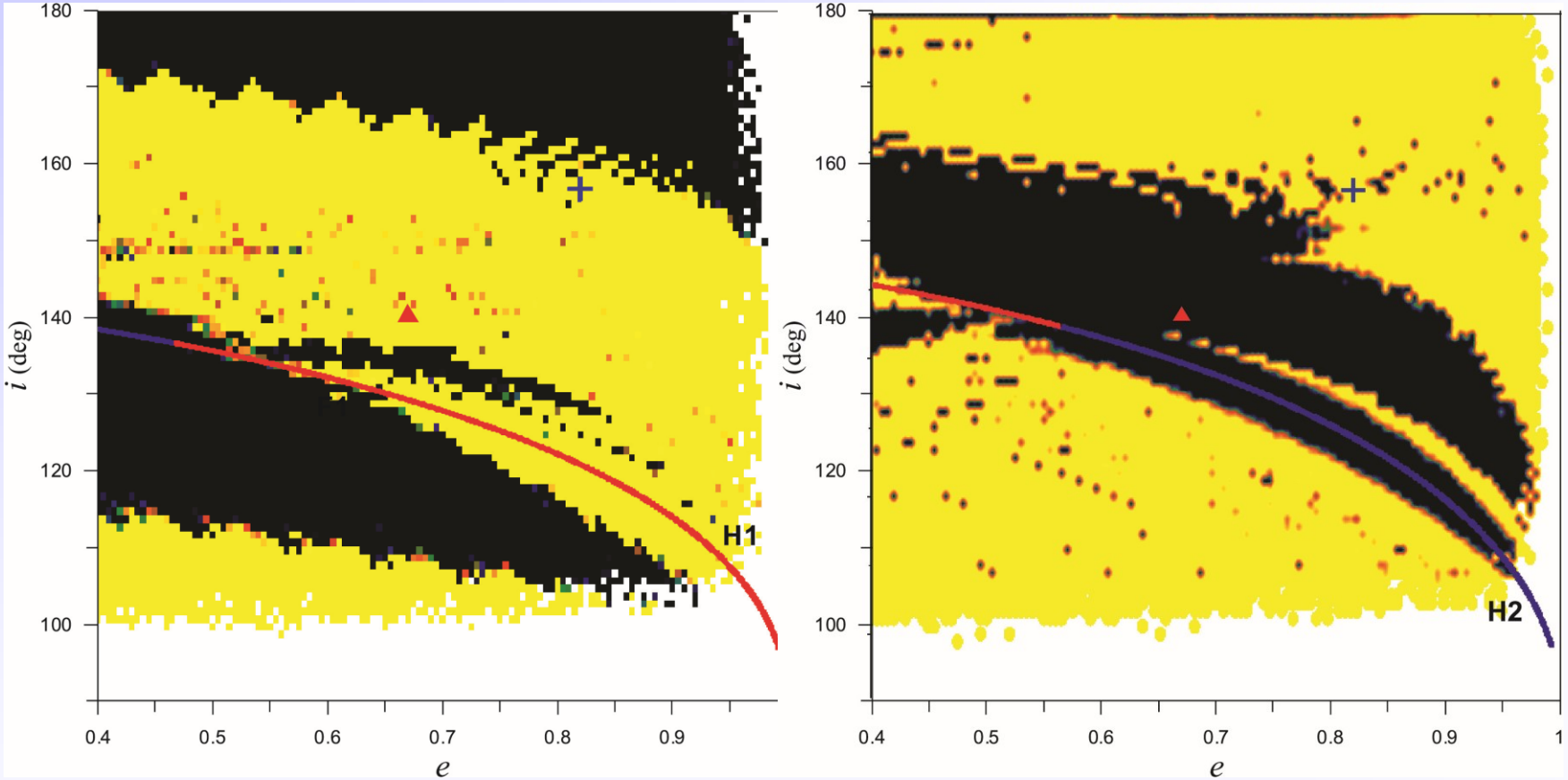

black colour→stability region, **yellow** colour→chaotic region,
"+" present position of asteroid, ▲averaged position of it along its evolution
(Kotoulas, Voyatzis and M.H.M. Morais: 2022a, PSS 210 (105374))

Evolution of the asteroid 2009 HC82 (343158 Marsyas)

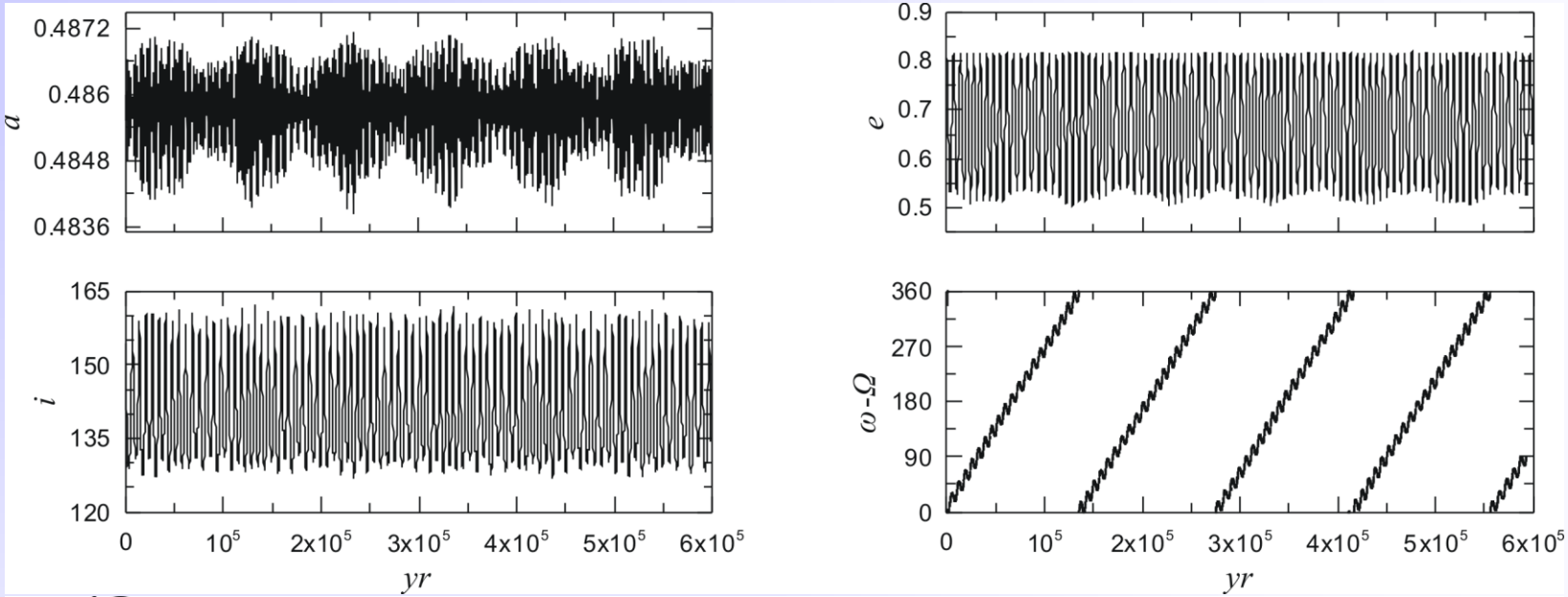

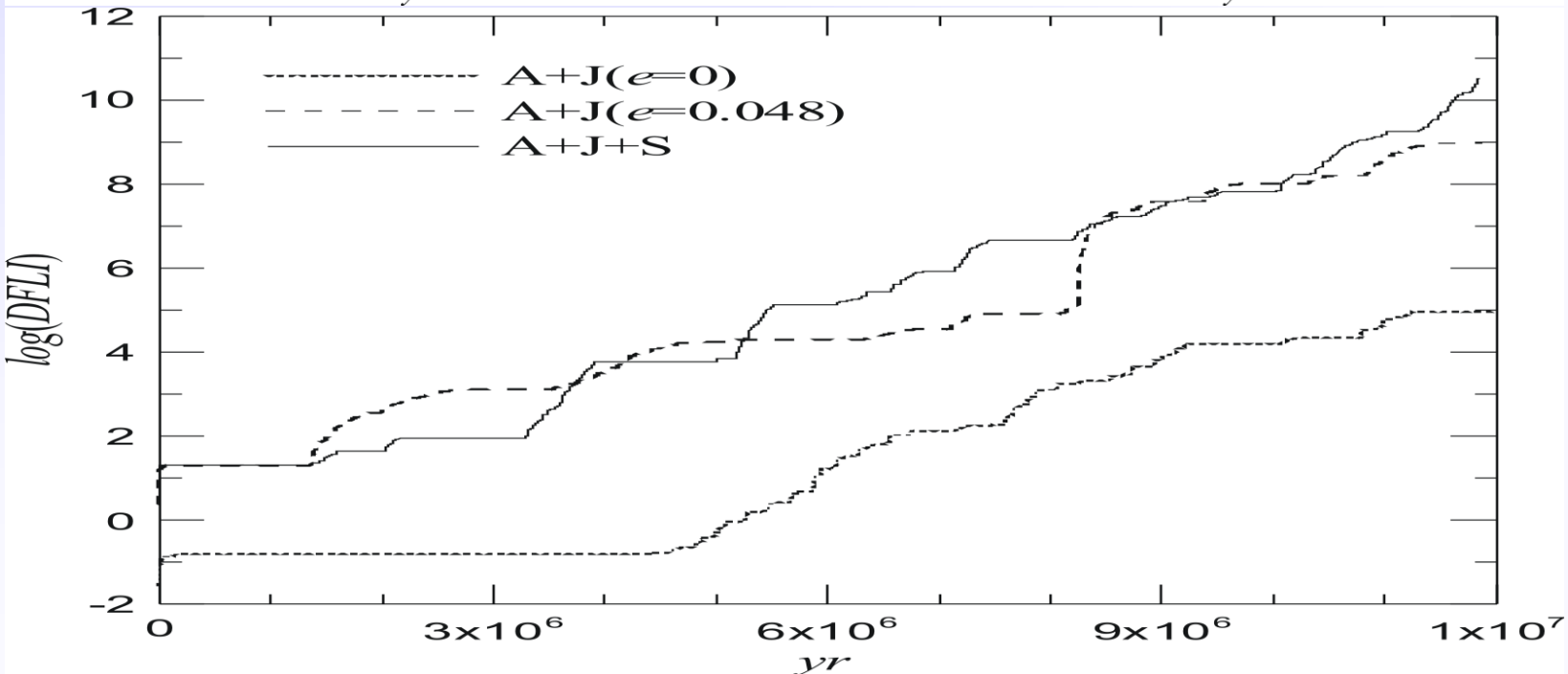

Third order resonances

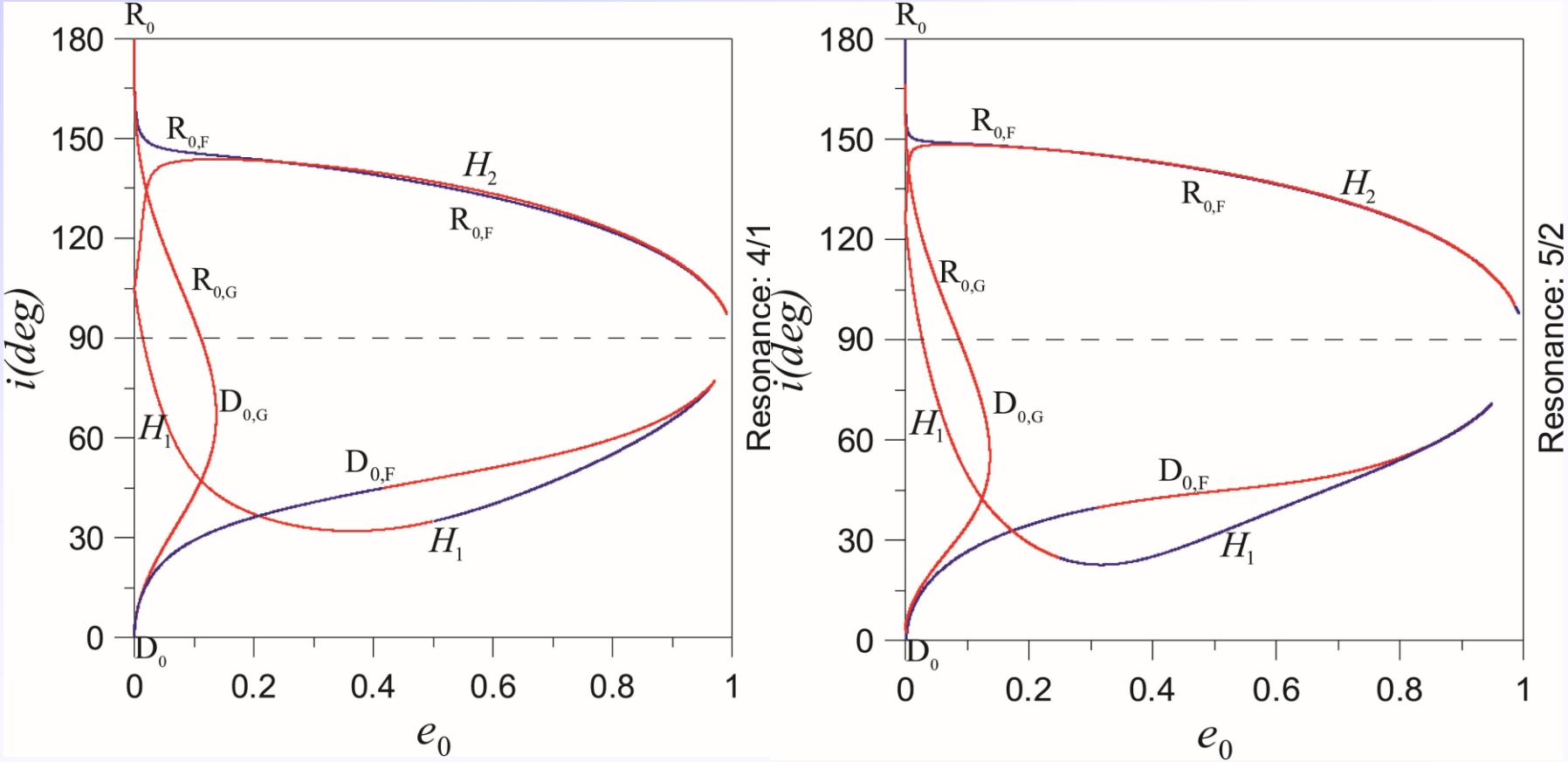

Conclusions

•Two families of symmetric retrograde periodic orbits in the planar circular problem: one is stable and the other one is unstable

•Bifurcation points from the planar circular to planar elliptic and to the three-dimensional circular one for all resonances of 1^{st}, 2^{nd} and 3^{rd} order between 2.0 and 4.5 A.U.

•Planar elliptic problem: in many cases one family is stable and the other one is unstable
•Stable POs→ surrounded by regular librations,
•Unstable POs→formation of phase space regions with chaotic motion.

•3D circular problem: both stable and unstable periodic orbits→ Families of retrograde periodic orbits are connected with families of direct orbits or terminate to collision orbits with Sun.

•The absence of asteroids in the main belt may be related with the existence of unstable periodic orbits

Publications

- T. Kotoulas and G. Voyatzis: 2020a, Planar retrograde periodic orbits of the asteroids trapped in two-body mean motion resonances with Jupiter, ***Planetary and Space Science*** **182**, 104846
- T. Kotoulas and G. Voyatzis: 2020b, Retrograde periodic orbits in 1/2, 2/3 and 3/4 mean motion resonances with Neptune, ***Celestial Mechanics and Dynamical Astronomy*** **132**:33
- M.H.M. Morais, F. Namouni, G. Voyatzis, T. Kotoulas: 2021, A study of the 1/2 retrograde resonance: periodic orbits and resonant capture, ***Celestial Mechanics and Dynamical Astronomy*** **133**:21
- T. Kotoulas, G. Voyatzis and M.H.M. Morais: 2022a, Three-dimensional retrograde periodic orbits of asteroids moving in mean motion resonances with Jupiter, ***Planetary and Space Science*** **210**, 105374
- T. Kotoulas, G. Voyatzis and M.H.M. Morais: 2022b, The phase space structure of higher order retrograde resonances with Neptune: The 4/5, 7/9, 5/8 and 8/13 cases, ***Celestial Mechanics and Dynamical Astronomy*** **134**, No. 6, pp. 1—25

G. Voyatzis and T. Kotoulas: 2023a, On the retrograde planar co-orbital asteroid motion with Jupiter ,
Complex Planetary Systems II –Kavli, IAU Symposium 382 –July 3-7, 2023, Namur, Belgium

Thank you!

email: tkoto@physics.auth.gr